Studies on ion selectivity of parchment impregnated Ba(II) molybdate artificial membrane

Afren Ansari[1], A.K. Shukla[1] and Mohd. Ayub Ansari[2]*

[1]Department of Chemistry, S.M.S. Govt. Model Science College, Gwalior-474009 (Madhya Pradesh), India
[2]Department of Chemistry, Bipin Bihari College, Jhansi-284001 (Uttar Pradesh), India
*Corresponding author E-mail:drayub67@gmail.com

Abstract

Parchment impregnated Ba(II) molybdate artificial membrane was prepared by the ion-interaction method using $BaCl_2$ and Na_2MoO_4 solutions. The prepared membrane was characterized by sophisticated instrumental techniques such as Scanning electron microscopy (SEM), Transmission electron microscopy (TEM), Fourier-transform infrared (FT-IR) spectroscopy, Thermogravimetric analysis (TGA)/Differential thermal analysis (DTA), X-ray diffraction (XRD) and Energy dispersive X-ray (EDX) analysis. The artificial membrane was tested for its antimicrobial activity against Gram-negative (*Escherichia coli* and *Pseudomonas aeruginosa*) and Gram-positive (*Staphylococcus aureus*) microorganism. The effective fixed charge density of the prepared membrane has been used individually to calculate theoretical bi-ionic potentials (BIP) and compared with experimentally determined values of bi-ionic potential. The selectivity of ions for the membrane has been found as $K^+>Na^+>Li^+$ which on the basis of the Eisenman-Sherry model of membrane selectivity, points towards the low field strength of the charge groups joined to the membrane matrix. Membrane conductance values has also been experimentally determined.

Keywords: *Parchment Impregnated Ba(II) Molybdate Membrane; Membrane Potential; Bi-ionic Potential; Membrane Conductance; Membrane Selectivity; Antimicrobial Activity.*

1. Introduction

Artificial membranes are used in many separation and purification processes and electrodialysis for saline water desalination [1-4]. Membranes are also used in many other processes such as fuel cell, power generation, energy saving, membrane electrolysis, electro-deionization etc. [5-7]. These membranes have found applications in foods, drugs, dairy industries, and in wastewater treatments due to their multipurpose nature. The electrochemical classification depends on the physical characteristic of membrane parameters like porosity, thickness, water absorption, transportation, ion exchange capacity etc. [8-9]. The potential observation of ions is a simple and influential method which is used to determine the transport property of ions across the charged membrane. The transport phenomenon of electrolyte ions through membrane system is very important process for the industrial application point of views [10-12].

The bi-ionic potential (BIP) is defined as a potential difference arising between the solutions of different electrolyte with same molar concentrations at a constant temperature and pressure when they are separated by a uniform charged membrane [13-15]. Depending on the transport mechanism or the assumption made in the derivation, the permeability ratio has been given various physical meaning as mobility ratio [16], ion exchange equilibrium constant [17], the product of the mobility ratio and Donnan ratio [18,19], the product of the mobility ratio and the distribution coefficient ratio [20], the product of the mobility ratio and ion exchange equilibrium constant [21,22] or the product of the equivalent conductance ratio and the ratio of partition coefficient [23]. Sandblom and Eisenman [23-25] have discussed the significance and implication of the observed permeability ratio.

This paper describes the preparation of parchment impregnated Ba(II) molybdate membrane and the effective fixed charge density of the membrane has been used individually to calculate theoretical bi-ionic potentials and compared with experimentally observed bi-ionic potential values. The values of membrane selectivity have calculated with the help of observed bi-ionic potential values and experimentally observed membrane conductance values. The membrane was tested in vitro for antimicrobial activity against clinically significant microorganisms such as *Escherichia coli*, *Pseudomonas aeruginosa* and *Staphylococcus aureus*. The new material was characterized by SEM, TEM, FT-IR Spectroscopy, TGA/DTA, XRD and EDX analysis.

2. Materials and method

Solutions of Li^+, Na^+, and K^+ chlorides of different concentrations were made. Na_2MoO_4 and $BaCl_2$ solutions of 99.90% of purity were prepared to make the $BaMoO_4$ precipitated material. All these reagents were of analytical grade and distilled water was used to prepare the solutions. Parchment paper (Amol Group of Companies, Mumbai, India) are also used.

2.1. Membrane preparation

Parchment impregnated Ba(II) molybdate artificial membrane was prepared by the method of interaction as suggested by Beg and coworkers [26]. First parchment paper was soaked in deionized water for about 2 hours and then tied to the flat mouth of a beaker containing 0.2M Na_2MoO_4 solution. The beaker was suspended for 72 hours in a porcelain dish having 0.2M solution of $BaCl_2$. The two solutions (fresh solution) were interchanged later and kept for another 72 hours. Thus parchment paper and inorganic precipitate as a whole acts as a artificial membrane. The membrane thus prepared was washed with deionized water to remove free electrolytes.

2.2. Measurement of membrane potential

The electrochemical cell of the type (Figure 1)
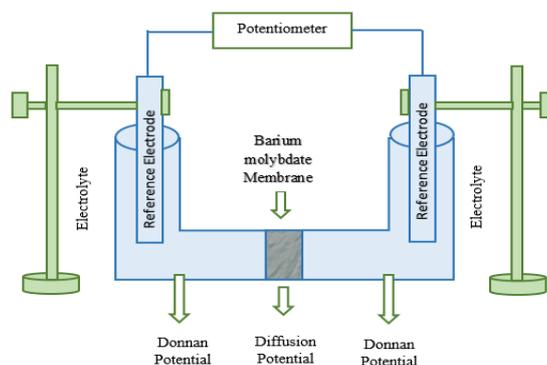
Fig. 1: Electrochemical Setup for Membrane Potential Measurements

was used for measuring membrane potential ($\Delta \psi$) arising through the membrane by maintaining a tenfold difference in concentration (C_2/C_1=10) and using a digital potentiometer (model 318, systronics). All the monovalent electrolytic solutions used in the investigation were prepared from analytical grade reagents and deionized water [27].

2.3. Measurement of bi-ionic potential

The bi-ionic potential was determined by setting up electrochemical cell of the type (Figure 2) and using a digital potentiometer (model 318, Systronics).
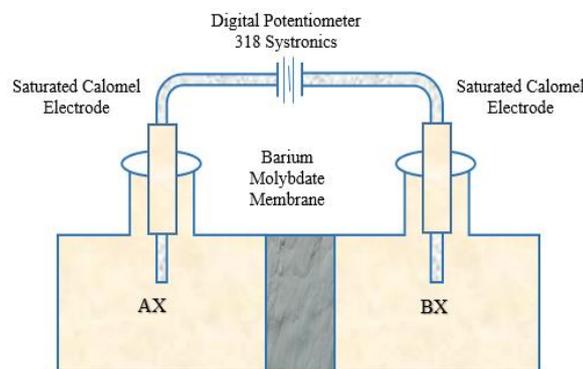
Fig. 2: Electrochemical Setup for Bi-ionic Potential Measurements

Aqueous solutions of Na^+, K^+ and Li^+ chlorides (BDH, AR grade) were used in the investigation. The solutions on both the sides of the membrane was vigorously stirred with a pair of electrically operated magnetic stirrers to remove complete or at least to minimize the effect of film control diffusion [28]. The whole cell was immersed in a water thermostate maintained at 25±0.1°C.

2.4. Characterization of the membrane

The performance of an ion exchange membrane is depends on its complete characterization, which involves the determination of all such parameters that affect its electrochemical properties. These parameters are the membrane water uptake, porosity, thickness, swelling etc. and was determined by Khan et al. [29].

2.4.1. Water uptake (% total wet weight), porosity, thickness, swelling, SEM, TEM, FT-IR, TGA/DTA, XRD and EDX studies of the parchment impregnated membrane

The prepared membrane was soaked in deionized water for 2 hour, blotted quickly with Whatman filter paper to remove surface moisture and immediately weighted. These were further dried to a constant weight in vacuum over P_2O_5 for 24 hour. Membrane porosity was determined as the volume of water incorporated in the cavities per unit membrane volume from the water uptake data. Membrane thickness was measured by taking the average thickness of the membrane by using screw gauge. Membrane swelling was measured as the difference between the average thickness of the membrane equilibrated in 1M NaCl solution for 24 hour and the dry membrane. The characterization, pore structure, micro/macro porosity, homogeneity, thickness, cracks and surface morphology of membrane was analyzed with SEM model

JSM-7100F Oxford. Gold Sputter coatings was carried out on the desired membrane sample at pressure 1 Pa. TEM analysis was carried out to indicate the particle size of parchment impregnated Ba(II) molybdate membrane. The TEM image of the membrane was obtained by a transmission electron microscope model Thermo Scientific™ Talos L120C.The FT-IR spectrum of membrane was taken by Bruker Tensor 27 spectrophotometer. The entrance and exit beams to the sample compartment were sealed with a coated KBr window and there was a hinged cover to seal it from the environment. The degradation process and thermal behaviour of the membrane was investigated using TGA under N_2 atmosphere using a heating rate of 20°C min^{-1} from 25 to 600°C and DTA using thermal analyzer Mettler-Toledo. The XRD pattern of the membrane was recorded by X-ray diffractometer (Panalytical X' pert Power) with Cu Kα radiation. The EDX spectrum of membrane was carried out on the scanning electron microscope (model JSM-7100F Oxford).

2.4.2. Antimicrobial activity of the parchment impregnated membrane

Antimicrobial activity of the parchment impregnated Ba(II) molybdate membrane was studied by well agar plate diffusion method according to Pandey et al. [30]. Antimicrobial activity test of the artificial membrane along with the solvent like THF as control was carried out using nutrient agar plates. All the organisms (*Escherichia coli*, *Pseudomonas aeruginosa* and *Staphylococcus aureus*) were grown separately in nutrient broth and incubated overnight at 37°C. After 12 hour the bacterial growths in nutrient broth were poured on the nutrient agar plates and allowed to stand for a minute. The excess cultures were removed after a while. Well was cut of the size of 8mm dia. to a depth of 8mm in this nutrient agar with the help of microtips (usually used with micropipette of 100 to 1000 micro litre). One well was cut at equal distance in each plate. The bottom of the well was sealed with a drop of fresh molten nutrient agar and allowed to stand for some time so that it solidified. The well was charged fully with the different preparations and incubated at 30°C for 24 hours. After 24 hour the plates were observed for the inhibition of bacterial growth with clear zones around the well. Diameter the clear zones were measured with the help a ruler and results recorded. The test was also performed along with different antibiotics like Cefotaxime, Augmentin, Chloramphenicol, ofloxacin, Co-Trimoxazole, Ciprofloxacin, Erythromycin, Gentamicin, Lincomycin, Penicillin G and Vancomycin against *Escherichia coli*, *Pseudomonas aeruginosa* and *Staphylococcus aureus* for their comparative study.

3. Results and discussion

The water uptake, porosity, thickness, and swelling results of parchment impregnated Ba(II) molybdate membrane are given in Table 1.

Table 1: Water uptake, Porosity, Thickness, and Swelling Properties of Parchment Impregnated Ba(II) Molybdate Artificial Membrane

Water uptake as % weight of wet membrane	1.086
Porosity (Φ)	0.0657
Thickness (cm)	1.055
Swelling (%)	0.99

The water uptake of a parchment impregnated artificial membrane depend on the vapour pressure of the surrounding. High order of water uptake, swelling and porosity with less thickness of membrane suggests that the diffusion across the membrane would occur mainly through exchange sites [31].

The SEM micrographs of parchment impregnated artificial membrane are appeared in Figure 3 (A to B). SEM images shows porosity, deviations and breakages or cracks on the surface of the membrane. Particles in the membrane are irregularly condensed and adopt a heterogeneous structure composed of masses of various sizes. SEM micrographs illustrated that the examined membrane has a porous surface and it helps the easy transportation of ions as well as charged species.

(A)   **(B)**
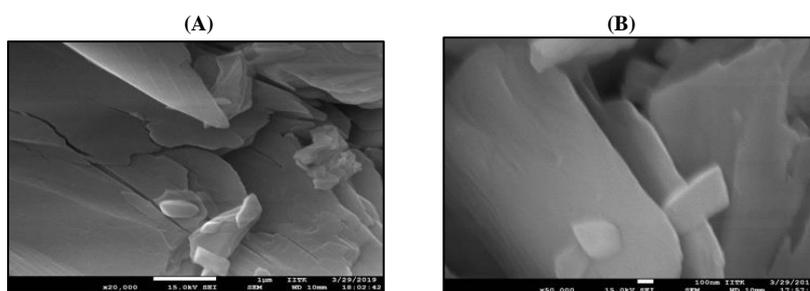
Fig. 3: (A to B): SEM Micrographs of Parchment Impregnated Ba(II) Molybdate Artificial Membrane

The TEM micrographs of the parchment impregnated artificial membrane are appeared in Figure 4 (A to B). It can be seen that the Ba(II) molybdate precipitate is consistently distributed on the surface of parchment paper. The particles size are 500 nm, which is slightly lower than that determined by SEM. TEM micrographs shows that the particle size is nanometer range would provide enhanced surface-to-volume ratio and hence a very small amount of the material would be sufficient to prepare the useful membrane.

(A)   **(B)**
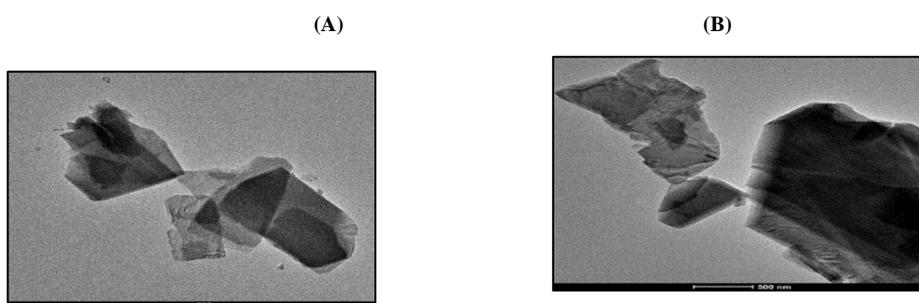
Fig. 4: (A to B): TEM Micrographs of Parchment Impregnated Ba(II) Molybdate Artificial Membrane

The FT-IR spectra of parchment impregnated membrane is shown in Figure 5. A strong intensity band at 3678.170 cm⁻¹ clearly indicate the presence of water molecules. The weak intensity bands at the range of 2368.49 cm⁻¹, 1676.07 cm⁻¹, 1573.85 cm⁻¹ and 887.22 cm⁻¹ showed the presence of carbon hydrogen bond, oxygen hydrogen bending vibration bond, metal halide bond and molybdenum oxygen double bond of the artificial membrane respectively.
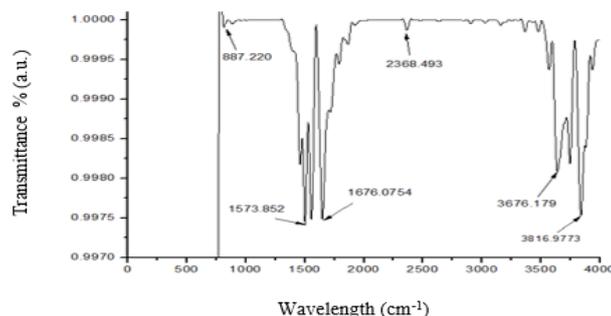
Fig. 5: FT-IR Spectra of Parchment Impregnated Ba(II) Molybdate Artificial Membrane

The TGA/DTA curve of parchment impregnated membrane is shown in Figure 6. The TGA curve of Ba(II) molybdate material indicates the weight loss in different temperature range up to 600°C. The first weight loss of 14.95 mg at the temperature 277.36°C and second weight loss of 14.51 mg at 324.59°C was found for parchment impregnated material. So it is clear that the gradual weight loss on increasing the temperature. Therefore, it is obvious that the material has some hydrophilic nature that could absorb moisture from the surrounding atmosphere.

There is also DTA curve specifying the parchment impregnated Ba(II) molybdate material showing temperature deduction at 217.26 and 271.04°C. Therefore the material shows endothermic nature which means that the heat changes must be there by deducing the temperature.
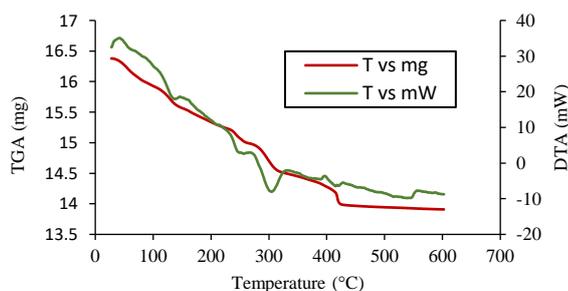
Fig. 6: TGA/DTA Curve of Parchment Impregnated Ba(II) Molybdate Artificial Membrane

The XRD spectra of the parchment impregnated membrane is shown in Figure 7, this shows sharp peaks of different intensity at different value of 2-Theta range. All high (8.650, 10.870 and 12.655) and less (34.858, 51.652 and 65.911) intense peaks are found from the range of 10-80˚ values which represented the examined material corresponds to some planes at different ranges. This analysis indicated that the parchment impregnated Ba(II) molybdate membrane has crystalline nature.
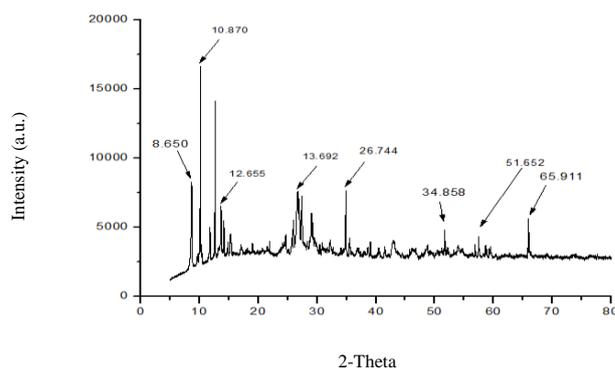
Fig. 7: XRD Pattern of Ba(II) Molybdate Parchment Impregnated Artificial Membrane

The EDX spectra of the membrane is appeared in Figure 8 and the result of ultimate analysis of synthesized membrane particles in this study are given in Table 2. The presence of chemical constituents (Mo, O, C, Ba, Na and Ti) in the EDX spectrum in respective ratios confirms the formation of parchment impregnated Ba(II) molybdate artificial membrane.

Fig. 8: SEM Supported EDX Spectrum of Parchment Impregnated Ba(II) Molybdate Membrane

Table 2: Elemental Analysis of Parchment Impregnated Ba(II) Molybdate Membrane Particle

Elements	% Wt.	σ (error)
Molybdenum	37.5	0.8
Oxygen	32.6	0.8
Carbon	15.5	1.0
Barium	10.9	0.6
Sodium	2.0	0.2
Titanium	1.5	0.2

The antimicrobial activity of parchment impregnated Ba(II) molybdate membrane was tested in vitro condition against two Gram-negative microbes *Escherichia coli* (K 12) and *Pseudomonas aeruginosa* (MTCC 2488) and one Gram-positive microorganism *Staphylococcus aureus* (MSSA 22) using well agar plate diffusion method. The membrane was tried to dissolve in THF. Hence whether this it has any antimicrobial activity, needs to be checked. Therefore this was used as control vis-a-vis the test proper. In any such experiment control value is a must for comparison.

Ba(II) molybdate membrane has highest inhibition against *Staphylococcus aureus* in comparison to *Escherichia coli*, *Pseudomonas aeruginosa* and control as shown in Table 3 and the results of different antibiotics are given in Table 4.

Table 3: Antimicrobial Activity of Parchment Impregnated Ba(II) Molybdate Membrane (With Zone of Inhibition in mm)

Microorganism	Ba(II) molybdate membrane	THF (as control)
Escherichia coli	13	13
Pseudomonas aeruginosa	13	14
Staphylococcus aureus	16	6

Table 4: Antimicrobial Activity of Standard Antibiotics

HIMEDIA : HX038		
Antibiotics	**Concentration**	***Escherichia coli***
Cefotaxime (CTX)	30 µg	17 mm dia
Augmentin (AMC)	30 µg	7 mm dia
Erythromycin (E)	10 µg	5 mm dia
Chloramphenicol (C)	30 µg	17 mm dia
Ofloxacin (OF)	5 µg	20 mm dia
Co-Trimoxazole (COT)	25 µg	20 mm dia
HIMEDIA : HX038		
Antibiotics	**Concentration**	***Pseudomonas aeruginosa***
Cefotaxime (CTX)	30 µg	20 mm dia
Augmentin (AMC)	30 µg	R (Resertant)
Erythromycin (E)	10 µg	7 mm dia
Chloramphenicol (C)	30 µg	8 mm dia
Ofloxacin (OF)	5 µg	25 mm dia
Co-Trimoxazole (COT)	25 µg	10 mm dia
HIMEDIA : HX090		
Antibiotics	**Concentration**	***Staphylococcus aureus***
Ciprofloxacin (CIP)	5 µg	17 mm dia
Erythromycin (E)	15 µg	7 mm dia
Gentamicin (GEN)	10 µg	22 mm dia
Lincomycin (L)	15 µg	21 mm dia
Penicillin G (P)	10 µg	26 mm dia
Vancomycin (VA)	30 µg	15 mm dia

The Table 4 indicates that the erythromycin with zone of inhibition as 5, 7, 7 millimeter diameter was less activity than the other standard antibiotics.

The erythromycin (of the concentration of 10, 10, 15 µg/disc, HiMedia) was less sensitive against the two Gram-negative and one Gram-positive microorganism (with zone of inhibition as 13, 13, 16 mm) respectively. It is observed that the prepared Ba(II) molybdate membrane has extraordinary inhibitory effect against the growth of microorganism.

Tetrahydrofuron (THF) as control did not show clear zone of inhibition of microbial growth in any plate as shown in Figure 9. Therefore, it is clear that the Gram-negative and Gram-positive microorganism with high antimicrobial activity suggests that the artificial membrane can be used as a potent antimicrobial agent.

Fig. 9: Diameter of Zone of Inhibition of Parchment Impregnated Ba(II) Molybdate Membrane, THF (As Control) and Standard Antibiotics

The total bi-ionic potential (BIP) for alkali metal ions of equal valence is given by the following equation:

$$E_{BIP} = \left(RT / FZ\right) \ln \bar{D}_i \, a'_i \, \bar{\lambda}_j / \bar{D}_j \, a'_j \, \bar{\lambda}_i \tag{1}$$

a'_i / a'_j, $\bar{D}_i / \bar{D}_j$, $\bar{\lambda}_i / \bar{\lambda}_j$ are denoted the activity ratio of solutions, diffusion coefficient of ions in membrane phase and the ratio of activity coefficient of ions; R, T, Z and F have their usual meaning. Equation (1) reduces to (2) Wyllie and Kannan [32].

$$E_{BIP} = \left(RT / FZ\right) \ln a'_i \, \bar{U}_i / a'_j \, \bar{U}_j \tag{2}$$

Provided $\bar{U}_i = \bar{U}_j$ and the diffusion are replaced by mobilities. Wyllie [32] expressed the intramembrane mobility ratio as

$$\bar{U}_i / \bar{U}_j = \bar{t}_i / \bar{t}_j = \bar{m}_i \bar{\lambda}_i / \bar{m}_j \bar{\lambda}_j \tag{3}$$

Where $\bar{t}_i / \bar{t}_j$ denotes the membrane transference ratio, $\bar{m}_i$ and $\bar{m}_j$ are the steady state equilibrium concentration of i and j in the respective junction zone. $\bar{\lambda}_i$ is the conductivity of the membrane when it is wholly in i form and $\bar{\lambda}_j$ is the conductivity of the membrane when it is wholly in j form. Furthermore, it was shown that $\bar{m}_i / \bar{m}_j = K_{ji}$, K_{ji} is the selectivity. This on substitution into equation (3) gives:

$$\bar{U}_i / \bar{U}_j = K_{ji} \left(\bar{\lambda}_i / \bar{\lambda}_j\right) \tag{4}$$

Thus the ratio of mobilities was related to the chemical and electrical properties of the membrane.

The values of bi-ionic potential across parchment impregnated Ba(II) molybdate membrane with various monovalent electrolyte combinations at same concentrations are given in Table 5 and plotted in Figure 10. Equation (2) was used to evaluate intramembrane mobility ratio $\bar{U}_i / \bar{U}_j$, the values of $\bar{U}_i / \bar{U}_j$ thus calculated are given in Table 6.

Table 5: Experimental Values of Bi-ionic Potential E_{BIP} (mV) Across Ba(II) Molybdate Membrane in Contact with Various Monovalent Electrolyte Ion Pairs at Same Concentration at 25±0.1°C

Concentration (mol/L)	Electrolyte Ion Pair		
	KCl-NaCl	KCl-LiCl	NaCl-LiCl
0.1/0.1	6.8	1.6	7.1
0.05/0.05	7.5	1.9	7.6
0.02/0.02	8.9	3.2	9.8
0.01/0.01	10.8	5.9	12.8
0.005/0.005	11.9	7.9	18.9
0.001/0.001	12.7	8.5	19.5
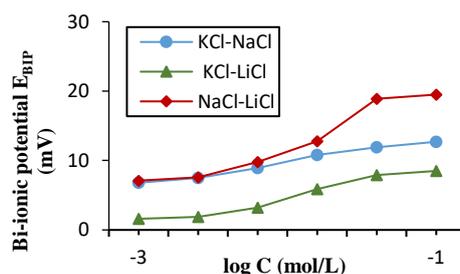
Fig. 10: Plots of Bi-ionic Potential E_{BIP} (mV) against log C (mol/L) for Ba(II) Molybdate Membrane Using Monovalent Electrolyte Ion Pairs

An interesting point with regard to the values of $\overline{U}_i / \overline{U}_j$ is that the mobility ratio undergoes considerable change with the concentration of the external solution. This behaviour was observable with each electrolyte pair.

Table 6: Values of the Intramembrane Mobility Ratio of Various Monovalent Electrolyte Ion Pairs Across Ba(II) Molybdate Membrane

Concentration (mol/L)	Electrolyte Ion Pair		
	$\overline{U}_{K^+} / \overline{U}_{Na^+}$	$\overline{U}_{K^+} / \overline{U}_{Li^+}$	$\overline{U}_{Na^+} / \overline{U}_{Li^+}$
	KCl-NaCl	**KCl-LiCl**	**NaCl-LiCl**
0.1/0.1	1.04	1.41	1.20
0.05/0.05	1.06	1.39	1.26
0.02/0.02	1.13	1.59	1.49
0.001/0.001	1.31	1.81	1.79
0.005/0.005	1.39	1.99	2.00
0.001/0.001	1.59	2.40	2.11

To gain knowledge of selectivity K_{ij} from the predetermined values of $\overline{U}_i / \overline{U}_j$ the ratio of electrical conductivities $\overline{\lambda}_i / \overline{\lambda}_j$, required in equation (4) must be known. Membrane conductance measurement was carried out when it was wholly in form i or form j. The values of membrane conductance at various salt concentrations are given in Table 7. The values are relatively more dependent on the concentration of the salts within the membrane as appeared in Figure 11. This implies that the membrane has a relatively high Donnan uptake of anion and a low selectivity constant value. The data of selectivity K_{ji} evaluated for the Ba(II) molybdate membrane from the ratio of their electrical conductivity and intramembrane mobility ratio using the data from Table 6-7 are given in Table 8. The intramembrane mobility ratio values also refer to the selectivity sequence of the membrane for the cations is $K^+>Na^+>Li^+$. This order of selectivity on the basis of the Eisenman-Sherry model of membrane selectivity [33, 34] points towards the weak field strength of the charged groups attached to the membrane matrix.

Table 7: Experimental Values of Membrane Electrical Conductance$\times 10^{-2}$ (mhos) Across Ba(II) Molybdate Membrane at 25$\pm$0.1°C

Concentration (mol/L)	Electrolytes		
	KCl	**NaCl**	**LiCl**
0.1/0.1	8.90	7.4	6.50
0.05/0.05	5.40	4.8	3.89
0.02/0.02	3.40	2.9	2.20
0.001/0.001	2.72	1.9	1.40
0.005/0.005	1.99	1.25	0.75
0.001/0.001	1.20	0.75	0.50
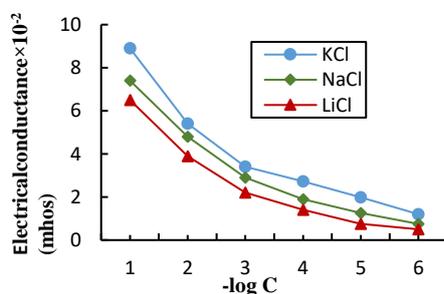
Fig. 11: Plots of Electrical Conductance (mhos) Against –log C for Ba(II) Molybdate Membrane

Table 8: Values of the Selectivity K_{ji} $\left(K_{ij} = 1/K_{ji} \right)$ Evaluated From Intramembrane Mobility Ratio and the Ratio of Electrical Conductivities at Various Electrolyte Concentration for Ba(II) Molybdate Membrane

Concentration (mol/L)	Selectivity		
	K$_{NaK}$	**K$_{NaLi}$**	**K$_{LiK}$**
0.1/0.1	0.91	1.06	1.09
0.05/0.05	0.99	1.09	1.13
0.02/0.02	1.00	1.38	1.42
0.001/0.001	1.19	1.59	1.49
0.005/0.005	0.99	1.36	1.72
0.001/0.001	1.41	1.69	1.49

According to Eisenman and Sandblom [25] derived the following equation (5)

$$P_i / P_j = K_{ji} \, \overline{U}_i / \overline{U}_j$$

(5)

Equation (5) suggests that the permeability ratio P_i / P_j can be calculated, provided that the mobility ratio $\overline{U}_i / \overline{U}_j$ and the ion exchange constant K_{ji} of a membrane for the ions are known the values of permeability ratio derived in this way from predetermined values of $\overline{U}_i / \overline{U}_j$ and K_{ji} for Ba(II) molybdate membrane are given in Table 9. The data in Table 9 show that the membrane is weakly selective and that the selectivity increases with a decrease in the concentration of the bathing solutions.

Table 9: Values of Permeability Ratio P_i / P_j of Various Monovalent Electrolyte to Pairs Across Ba(II) Molybdate Membrane

Concentration (mol/L)	Permeability ratio		
	P_{K^+} / P_{Na^+}	P_{K^+} / P_{Li^+}	P_{Na^+} / P_{Li^+}
0.1/0.1	0.89	1.30	1.37
0.05/0.05	0.96	1.37	1.47
0.02/0.02	1.09	1.89	1.99
0.001/0.001	1.37	2.48	2.78
0.005/0.005	1.52	2.99	2.96
0.001/0.001	1.97	3.61	3.99

The e.m.f. (bi-ionic potential) of the cell of the type shown in the experiment part has been related to the fixed charge concentration (φx) by the equation:

$$E_{BIP} = (RT / F) \ln \frac{\sqrt{1+(\varphi x M_A / 2a)^2} - (\varphi x M_A / 2a)}{\sqrt{1+(\varphi x M_B / 2a)^2} - (\varphi x M_B / 2a)} \tag{6}$$

Where $\varphi x M_A$ and $\varphi x M_B$ are the concentrations of the fixed ions on the membrane phase. Equation (6) can be used to calculate BIP across a membrane provided effective fixed charge density of the membrane and the concentration of external salt solutions are known. The values of BIP thus derived using pre-determined values of effective fixed charge density of the membrane [35] are given in Table 10. For comparison the observed values are also given in the same table. These values are closer to each other.

Table 10: Theoretically and Experimentally Observed Bi-ionic Potential E_{BIP} (mV) Values Across Ba(II) Molybdate Membrane at 25±0.1°C

Concentration (mol/L)	Electrolyte ion pairs					
	Experimental			Theoretical		
	KCl- NaCl	KCl -LiCl	NaCl -LiCl	KCl- NaCl	KCl- LiCl	NaCl-LiCl
0.1/0.1	6.8	1.6	7.1	6.1	1.2	6.3
0.05/0.05	7.5	1.9	7.6	6.9	2.2	7.8
0.02/0.02	8.9	3.2	9.8	9.3	3.1	11.4
0.001/0.001	10.8	5.9	12.8	11.3	6.1	12.9
0.005/0.005	11.9	7.9	18.9	12.8	8.0	18.7
0.001/0.001	12.7	8.5	19.5	13.2	8.9	19.7

It is well known that bi-ionic potential is a measure of selectivity [36] of membrane for ions of the same sign. Equation (7) has been found to predict the values of bi-ionic potential similar to equation (1) provided $\bar{\gamma}_B / \bar{\gamma}_A$ remains constant:

$$E_{BIP} = \frac{RT}{F} \ln \frac{\bar{U}_A \, a_A' \, \bar{\gamma}_B}{\bar{U}_B \, a_B' \, \bar{\gamma}_A} \tag{7}$$

This equation can be written as

$$E = \frac{RT}{F} \ln \frac{\bar{U}_A \, a_A'}{\bar{U}_B \, a_B'} \qquad (if \ \bar{\gamma}_A = \bar{\gamma}_B) \tag{8}$$

and

$$E_{BIP} = \frac{RT}{F} \ln \frac{\bar{t}_A}{\bar{t}_B} \tag{9}$$

Where

Provided that the Donnan ratio $\dfrac{\bar{a}_A}{a_A'} = \dfrac{\bar{a}_B}{a_B'}$ is established.

The bi-ionic potentials generated across parchment impregnated membrane was measured keeping the concentration of AX constant and by varying concentration of BX, and again by keeping BX constant and varying AX. These measurements were extended to three solution pairs, i.e. KCl-NaCl, NaCl-LiCl and KCl-LiCl. The bi-ionic potentials thus measured are given in Table 11. These values are also appeared in Figure 12 as a function of a_{AX} / a_{BX} .

Table 11: Experimental Values of Bi-ionic Potential across Parchment Impregnated Ba(II) Molybdate Membrane Keeping the Concentration of One Electrolyte Constant and Varying the Concentration of Other Salt and Vice-Versa

Concentration (mol/L)	Electrolyte ion pairs					
	KCl-NaCl	NaCl-KCl	NaCl-LiCl	LiCl-NaCl	KCl-LiCl	LiCl-KCl
0.1/0.5	9.4	1.0	11.3	-6.9	10.4	-4.0
0.1/0.01	15.9	-10.0	21.8	-21.9	18.8	-16.8
0.1/0.005	23.0	-19.3	32.1	-34.5	27.5	-27.9
0.1/0.001	30.0	-28.6	41.9	-45.8	36.3	-38.5
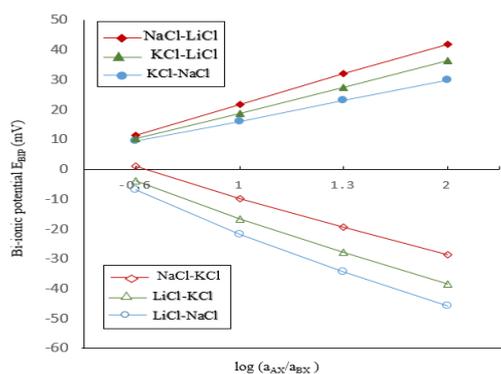
Fig. 12: Plots of Bi-ionic Potential E_{BIP} (mV) Against log (a_{AX} / a_{BX}) for Ba(II) Molybdate Membrane

Good straight lines demanded by equation (8) are obtained. The potential of intersection of the two straight lines at the same activity, i.e. a_{AX} / a_{BX} = 1, gives the value of transport ratio using equation (9). The transport ratio, thus obtained for different monovalent electrolyte pairs for the Ba(II) molybdate membrane are given in Table 12.

Table 12: Transport Ratio Obtained for Different Monovalent Electrolyte Ion Pairs Across the Parchment Impregnated Ba (II) Molybdate Membrane

Membrane	Transport ratio		
	$\bar{t}_{K^+}$ / $\bar{t}_{Na^+}$	$\bar{t}_{K^+}$ / $\bar{t}_{Li^+}$	$\bar{t}_{Na^+}$ / $\bar{t}_{Li^+}$
Ba(II) Molybdate	1.15	1.08	1.06

These results also point towards the order of selectivity of cations transporting through the membrane which is as follows:

$K^+ > Na^+ > Li^+$

4. Conclusion

The parchment impregnated Ba(II) molybdate membrane was successfully fabricated by using ion-interaction method. The values of bi-ionic potential across the membrane using various combinations of monovalent electrolytes at same concentrations was measured based on the Non-equilibrium thermodynamics. The selectivity of ions for the membrane has been found as $K^+ > Na^+ > Li^+$ which on the basis of the Eisenman-Sherry model of membrane selectivity, points towards the low field strength of the charge groups joined to the membrane matrix. The conductivity of the membrane in contact with single salt was also determined experimentally in order to evaluate the selectivity of the membrane using the predetermined data of intramembrane mobility ratio. The electrochemical parameters are the most important factors which help to show the good results of an ideal ion-selective membrane. The antimicrobial results indicate that the Gram-negative and Gram-positive microorganism show high activity which leads that the artificial membrane can be used as a potent antimicrobial agent. Therefore Ba(II) molybdate membrane can be used for several industries, including water treatment for domestic and industrial water supply, chemical, pharmaceutical, biotechnological, beverages, food, and other separation processes.

Acknowledgement

References

[1] A.A. Khan, M.M. Alam (2004), New and novel organic–inorganic type crystalline 'polypyrrolel/polyantimonic acid' composite system: Preparation, characterization and analytical applications as a cation-exchange material and Hg (II) ion-selective membrane electrode, Anal. Chim. Acta, 504, 253–264. https://doi.org/10.1016/j.aca.2003.10.054.

[2] A.A. Khan, M.M. Alam (2003), Synthesis, characterization and analytical applications of a new and novel 'organic–inorganic' composite material as a cation exchanger and Cd(II) ion-selective membrane electrode: Polyaniline Sn(IV) tungstoarsenate, React. Funct. Polym., 55, 277–290. https://doi.org/10.1016/S1381-5148(03)00018-X.

[3] K.A. Shandi, F.A. Wedian (2009), Estimation of composition, coordination model, and stability constant of some metal/phosphate complexes using spectral and potentiometric measurements, Chem. Pap., 63, 420–425. https://doi.org/10.2478/s11696-009-0027-5.

[4] Peng Jing, A. Zawodzinski Thomas (2020), Describing ion exchange membrane-electrolyte interactions for high electrolyte concentrations used in electrochemical reactors, Journal of Membrane Science, 593, 117340. https://doi.org/10.1016/j.memsci.2019.117340.

[5] R. Scherer, A.M. Bernardes, M.M.C. Forte, J.Z. Ferreira, C.A. Ferreira (2001), Preparation and physical characterization of a sulfonated poly(styrene-co-divinylbenzene) and polypyrrole composite membrane, Mater. Chem. Phys., 71, 131–136. https://doi.org/10.1016/S0254-0584(00)00515-0.

[6] Chenhao Ji, Cheng-Wei Lin, Shenghao Zhang, Yaoli Guo, Zhe Yang, Weiping Hu, Shuangmei Xue, Q. Jason Niu and Richard B. Kaner (2022), Ultrapermeable nanofiltration membranes with tunable selectivity fabricated with polyaniline nanofibers, Journal of materials chemistry A, Issue 8, https://doi.org/10.1039/D1TA10898K.

[7] Arsalan Mohd, Imteyaz Shahla, Zeeshan Mohd, Rafiuddin (2015), Synthesis, characterization, and electrochemical observation of PVC-supported strontium tungstate inorganic precipitated composite membrane, Desalination and Water Treatment, 57, 1–11. https://doi.org/10.1080/19443994.2015.1080191.

[8] M. Arsalan, Rafiuddin (2014), Binding nature of polystyrene and PVC 50:50% with CP and NP 50:50% ion exchangeable, mechanically and thermally stable membrane, J. Ind. Eng. Chem. 20, 3283–3291. https://doi.org/10.1016/j.jiec.2013.11.068.

[9] Hao Pingjiao, J.G. Wijmans (2020), Effect of pore location and pore size of the support membrane on the permeance of composite membranes, J. of membrane science, 594, 117465. https://doi.org/10.1016/j.memsci.2019.117465.

[10] Zoheb Karim, Susanna Monti, Giovanni Barcaco, Anna Svedberg, Mohd Ayub Ansari, Sadaf Afrin (2020), Enhanced sieving of cellulosic microfiber membranes via tuning of interlayer spacing, Environ. Sci., Nano, 7, 2941-2952. https://doi.org/10.1039/D0EN00613K.

[11] K.P. Singh, R.K. Prajapati, S. Kumar and Mohd. Ayub Ansari (2010), Preparation of isoproturon and 2, 4-Dichlorophenoxyacetic acid imprinted membrane: Ion transport study, Desalination and Water Treatment, Vol. 24, 176-189. https://doi.org/10.5004/dwt.2010.1497.

[12] Afren Ansari, A.K. Shukla, Mohd. Ayub Ansari (2021), Preparation, Characterization and Electrical Conductance Studies of Inorganic Precipitate Parchment Supported Barium Molybdate Membrane, Materials Today: Proceeding, 47,5, 522, https://doi.org/10.1016/j.matpr.2021.03.302.

[13] F.A. Siddiqi, N. Lakshminarayanaiah, M.N. Beg (1971), Studies with inorganic precipitate membranes. III.[†] Consideration of energetics of electrolyte permeation through membranes, J. Polym. Sci., 9, 2869–2875. https://doi.org/10.1002/pol.1971.150091009.

[14] R.S. Kushwaha, Mohd. Ayub Ansari & R. Tiwari (2001), Transport studies of parchment supported model membrane: Test of bi-ionic potential theories and evaluation of membrane selectivity for metal ions, Indian journal of chemistry, Vol 40A, pp. 270-274.

[15] Mohd Rashid, Sher Ali and Mohd. Ayub Ansari (2013), Bi-ionic potential studies on parchment supported synthetic membranes, Der Chemica Sinica, 4, 97-106.

[16] M. Planck, Z. Phys. (1891), Allgemeines zur neueren Entwicklung der Wärmetheorie, Chem., 8, 647. https://doi.org/10.1515/zpch-1891-0848.

[17] Armineh Hassanvand ,Wei Kajia, Talebi Sahar, Q. Chen George and E. Kentish Sandra (2017), The Role of Ion Exchange Membranes in Membrane Capacitive Deionisation, Membranes, 7, 54, 1-23. https://doi.org/10.3390/membranes7030054.

[18] KM Elsherif, El-Dali Abdelmeneim, El-Hashani Ashraf, Musa Mohamed (2014), Ion Selectivity Across Parchment-Supported Silver Chloride Membrane in Contact with Multi-valent Electrolytes, International Journal of Analytical and Bioanalytical Chemistry, 4(2), 58-62.

[19] Zehra Aiman & Mohammad Mujahid Ali Khan & Rafiuddin (2021), Modified composite cation exchange membrane with enhanced stability and electrochemical performance, Journal of Solid State Electrochemistry, 25, 1-16. https://doi.org/10.1007/s10008-020-04821-w.

[20] Mohd. Zeeshan, Rais Ahmad, Asif Ali Khan, Aftab Aslam Parwaz Khan, C. Bazan Guillermo, Basma Ghaleb Alhogbi, Hadi M. Marwani and Sakshi Singh (2021), Fabrication of a lead ion selective membrane based on a polycarbazole Sn(IV) arsenotungstate nanocomposite and its ion exchange membrane (IEM) kinetic studies, RSC Adv., 11, 4210. https://doi.org/10.1039/D0RA07534E.

[21] F. Helfferic (1962), Ion Exchange, McGraw Hill, New York.

[22] G. Karreman and G. Eisenman (1962), Electrical potentials and ionic fluxes in ion exchangers: I. "*n* type" non-ideal systems with zero current, Bull. Math. Biophys, 24, 413. https://doi.org/10.1039/D0RA07534E.

[23] G. Eisenman, J.A. Dani, J. Sandblom (1985), Recent Studies on the Energy Profiles Underlying Permeation and Ion-Selectivity of the Gramicidin and Acetylcholine Receptor Channel, Ion Measurement in Physiology and Medicine pp. 54-66. https://doi.org/10.1007/978-3-642-70518-2_9.

[24] J. Sandblom and F. Orme (1972), in "Membranes" (G. Eisenman, ed.), Dekker, New York, Vol. 1, 125.

[25] G. Eisenman, J. Sandblom, E. Neher (1978), Interactions in cation permeation through the gramicidin channel. Cs, Rb, K, Na, Li, Tl, H, and effects of anion binding, Biophys.,J., Vol 22, issue 27, pp. 307-340. https://doi.org/10.1016/S0006-3495(78)85491-5.

[26] M.N. Beg, F.A. Siddiqi, R. Shyam (1977), Studies with inorganic precipitate membranes: part XIV. Evaluation of effective fixed charge densities, Can J. Chem., 55, 1680-1686. https://doi.org/10.1139/v77-237.

[27] KM Elsherif, A. El-Hashani and A. El-Dali (2013), Potentiometric Determination of Fixed Charge Density and Permselectivity for Silver Thiosulphate, membrane Journal of Applicable Chemistry, 2, 1543.

[28] Elsherif Khaled Muftah, Ashraf El-Hashani, Abdelmeneim El-Dali, Rajab El-kailany (2014), Bi-ionic Potential Studies for Silver Thiosulphate Parchment-Supported membrane, International journal of advanced scientific and technical research, volume 1, 638-646.

[29] A.A. Khan, Inamuddin and A. Khan (2007), Preparation and characterization of a new organic-inorganic nano-composite poly-o-toluidine Th(IV) phosphate: Its analytical applications as cation-exchanger and in making ion-selective electrode, Talanta, 72, 699-710. https://doi.org/10.1016/j.talanta.2006.11.044.

[30] A. Pandey, I. Ali, K.S. Butola, T. Chatterji (2011), Isolation and characterization of actinomycetes against pathogen, Inter. J. appl. Biol. Pharma. Technol., 2, 384-392.

[31] Mohd Arsalan, Zehra Aiman, Mohammad Mujahid Ali Khan (2019), Preparation and characterization of polyvinyl chloride based nickel phosphate ion selective membrane and its application for removal of ions through water bodies. Groundwater for Sustainable Development, 8, 41-48. https://doi.org/10.1016/j.gsd.2018.06.008.

[32] Wyllie, M. R. J., Kannan S.L (1954), the Fundamentals of Electric Log Interpretation, Academic Press, N. Y.

[33] Eisenman G., Membrane Transport and Metabolism, Kleinzer A., Kotyk A., Eds, Academic New York, 163 (1961); Biophys. J. Suppl. 2 (1962) 259. https://doi.org/10.1136/bmj.2.5299.259-b.

[34] H. Sherry (1968), In Ion Exchange, Marinsky J.A.; in Ed., Dekker, New York, P. 2.

[35] T. Xu, K. Hu (2004), Separation and Purification Technology, 40, 231-236. https://doi.org/10.1016/j.seppur.2004.03.002.

[36] N. Lakshminarayanaiah (1969), Transport Phenomena in Membranes, Academic Press, New York.